A Test System Meeting Requirements under Normal and Contingency Conditions at Multiple Loadings for Transmission Expansion Planning

Bhuban Dhamala Student Member, IEEE, and Mona Ghassemi, Senior Member, IEEE

Zero Emission, Realization of Optimized Energy Systems (ZEROES) Laboratory

Department of Electrical and Computer Engineering, The University of Texas at Dallas, Richardson, TX, USA bhuban.dhamala@utdallas.edu, mona.ghassemi@utdallas.edu

Abstract—This paper introduces a high-voltage test system tailored specifically for transmission expansion planning (TEP). The network incorporates long transmission lines, and the line series impedance and shunt admittance for each line are computed utilizing the equivalent π circuit model for long transmission lines to account for the distributed nature of line parameters. The proposed test system offers technically feasible load flow solutions under normal and all single contingency conditions for three distinct loading scenarios: peak, dominant, and light loading conditions. As the real power system is subject to various loading scenarios and should be effectively operable under all conditions, this test system accurately replicates the properties of real power systems. The test system introduced in this paper can be a valuable resource for TEP research.

Keywords— Power System, test system, transmission expansion planning, load flow analysis, single contingency conditions, peak loading, dominant loading, light loading

I. INTRODUCTION

According to the International Energy Outlook report of 2023 between 2022 to 2050 [1], global energy consumption is expected to increase by up to 62% in the industrial sector, approximately 41% in the transportation sector, and three-fold between 2022 and 2050 in commercial and industrial infrastructure. The report also indicates that global electricity generation will also increase in the range of 30 to 76% compared to the year 2022, with this growth primarily supported by zero-carbon technologies, driven by mandated Renewable Portfolio Standards (RPS) aimed at reducing carbon emissions [2]. Achieving this ambitious goal in the U.S. by 2050 requires the capacity of high-voltage transmission lines to triple compared to 2023 levels [3]. This demands huge investment and extensive study in Transmission Expansion Planning (TEP) Studies. For effective expansion planning analysis, having a base test system is crucial. This system serves as a model for analysis and assessment, enabling the study of planning scenarios and the benchmarking of different TEP approaches for practical implementation.

Commonly used test cases in power system analysis and research are IEEE test cases [4] due to their long history in power systems. Despite having many IEEE test cases, their low voltage level, short transmission line length, and single-loading scenario do not mimic real power systems. Many synthetic power grid test cases with very large sizes having the

characteristics of real power systems are publicly available [4, 5]. However, these test systems are specifically designed for single loading condition without specifying the loading scenarios, such as peak loading conditions or other potential loading scenarios. Additionally, the capabilities of the existing test system to operate under all single contingency conditions are not clearly communicated. If the transmission expansion planning studies cannot ensure a technically feasible solution across different loading scenarios and under all single contingencies for each loading condition, it hinders the achievement of both technically and economically winning results from transmission expansion planning studies on that system. Moreover, available real or synthetic test systems for transmission expansion planning do not provide clear information on the length of the transmission lines in the power network and their line parameters. It is necessary to know the distance between buses or the length of lines in the existing test system to estimate the distance between new buses planning to be connected to the network. These aspects are crucial for accurately reflecting real power system conditions and conducting effective transmission expansion planning studies. This paper presents a fictitious 500 kV test system network tailored for transmission line expansion planning studies, incorporating long transmission lines for high voltage systems to mimic the real power system. The test system is designed to function seamlessly under normal and all single contingencies across various loading conditions, ensuring compliance with voltage, reactive power generation, and line loading criteria. Section II offers an overview of the test system, section III presents transmission line configuration and modeling, while sections IV and V delve into the problem formulations and detailed load flow analysis respectively. Section VI concludes the paper, highlighting the contributions.

II. OVERVIEW OF TEST SYSTEM

A. Network Topology

The single-line diagram depicted in Fig. 1 illustrates the proposed test system, which encompasses 17 buses and operates at a voltage level of 500 kV. These 17 buses consist of a slack bus (designated as bus 1), along with seven generator buses (buses 3, 6, 8, 10, 12, 13, and 15), and eight load buses. Table I provides the length of each transmission line within the system. The system incorporates long transmission lines connecting the buses to facilitate the transmission of power

This work was supported in part by the National Science Foundation (NSF) under Award #2306098.

over the long distance between them. These transmission lines vary in length, ranging from 261.30 km for line 11-13 to 458.18 km for line 14 -15.

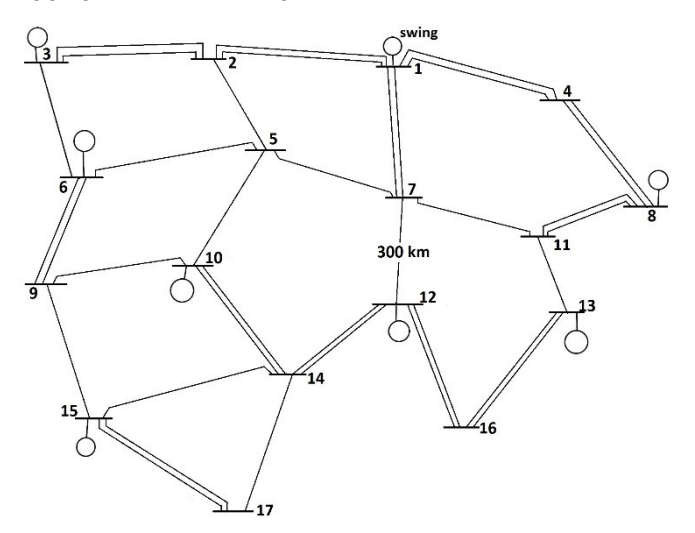


Fig. 1. Single line diagram of the 17-bus test system.

TABLE I. INFORMATION ON TRANSMISSION LINE LENGTH

Line	Length (km)	Line	Length (km)
1-2	410.33	7-12	300.05
1-4	426.78	8-11	349.10
1-7	370.92	9-10	447.28
2-3	436.90	9-15	398.20
2-5	294.56	10-14	392.74
3-6	349.56	11-13	261.30
4-8	416.14	12-14	348.37
5-6	415.00	12-16	406.46
5-7	435.50	13-16	417.27
5-10	376.35	14-15	458.18
6-9	316.35	14-17	403.64
7-11	387.10	15-17	402.16

B. Generation and Load Information

Detailed information on generation, information, and the required shunt capacitors at peak loading conditions are presented in Table II.

TABLE II. GENERATION, LOAD, AND SHUNT COMPENSATION INFORMATION AT PEAK LOAD

Bus	V (p.u)	Type	P _g (MW)	P _L (MW)	Q _L (MW)	Shunt Capacitor
1	1.05	Slack				
2	-	PQ	-	1900.00	920.21	100 Mvar
3	1.03	PV	3600	1750.00	847.56	-
4	-	PQ	-	1850.00	896.00	100 Mvar
5	-	PQ	-	1600.00	774.92	150 Mvar
6	1.03	PV	3600	1700.00	823.34	-
7	-	PQ	-	1900.00	920.21	-
8	1.04	PV	3600	1600.00	774.92	-
9	-	PQ	-	2000.00	968.64	400 Mvar
10	1.03	PV	3600	1700.00	823.34	-
11	-	PQ	-	1800.00	871.77	200 Mvar
12	1.05	PV	3600	1600.00	774.92	-
13	1.05	PV	3600	1800.00	871.77	-
14	-	PQ	-	2300.00	1113.94	-
15	1.00	PV	3500	1700.00	823.35	-
16	-	PQ	-	1750.00	847.56	50 Mvar
17	-	PQ	-	1150.00	556.97	150 Mvar

Bus 1 is the slack bus and its voltage magnitude and voltage angle are set to $|V_1|=1.05$ p.u and $\delta_1=0$. The voltage settings of other generators and their respective active power generation capacity are illustrated in the Table. The system has sixteen loads connected to all voltage-controlled buses and the load buses and each load has 0.9 lagging power factors. At peak loading condition, a total of 1150 Mvar fixed shunt capacitors are connected at different buses.

III. TRANSMISSION LINE

A. Transmission Line Configuration

The transmission line configuration for the proposed 500 kV test system, as illustrated in Fig. 2, features horizontal arrangements with a phase spacing of 12.3 m, while ensuring the minimum sub-conductors height of 24 m from the ground level. Each phase consists of four sub-conductors with a spacing of 0.45 m arranged in circular form. This tower configuration for a 500 kV transmission line is selected from the reference [7]. The Macaw conductors, with an outer diameter of 1.045 inches and a current carrying capacity of 870 Amperes, serve as the designated sub-conductor. In a double-circuit line, each circuit holds the same line configuration. For instance, the two lines connecting buses 1 and 2 are situated in two different towers with the same configuration as shown in Fig. 2.

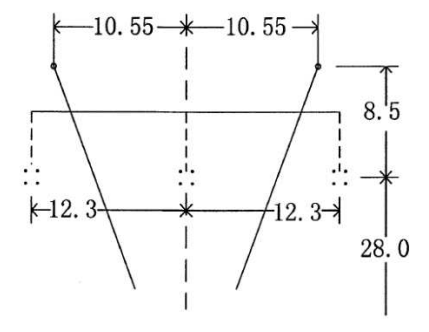


Fig. 2. 500 kV transmission Line configuration used in the test system.

B. Transmission Line Paramters

The line parameters of transmission lines encompass a range of electrical attributes delineating the line's performance in transmitting electrical energy. For a given number of bundle conductors per phase denoted as b, these parameters can be computed as

$$R_{eq} = \frac{R}{b} \Omega/\text{km} \tag{1}$$

$$x = 2\pi f \times 2 \times 10^{-7} \ln \left(\frac{GMD}{r'} \right) \Omega / \text{km}$$
 (2)

$$x = 2\pi f \times 2 \times 10^{-7} \ln\left(\frac{GMD}{r'}\right) \Omega/\text{km} \qquad (2)$$
$$y = 2\pi f \frac{2\pi \varepsilon_0}{\ln\left(\frac{GMD}{r_0}\right)} \qquad S/km \qquad (3)$$

where f represents the system frequency, ε_0 denotes the permittivity of free space, and GMD stands for the geometric mean distance. When dealing with bundled conductors, the parameters r' and r_0 should be substituted with the equivalent bundle radiuses for inductance calculations and capacitance calculations.

C. Modeling of Transmission Line

In the case of long transmission lines, relying solely on the multiplication of per unit length line parameters by the transmission line length to calculate the total line impedance and shunt admittance leads to inaccuracies. As the length of the transmission line increases, the error in estimating these parameters just by scaling them with distances also increases. The details of the percentage difference in resistance, reactance, and susceptance based on the just-by scaling with line length compared to the actual parameters are depicted in Fig. 3. This result shows that the difference in resistance and the inductive reactance is remarkable for the line having length more than 150 miles.

Therefore, the accurate modeling of a long transmission line necessitates uniform distribution of the line parameters throughout the line length. Analyzing such lines directly using distributed parameter models can be computationally intensive. The Pi model simplifies this analysis by condensing the distributed parameters into lumped elements and can provide a simplified and accurate representation of long transmission lines. The equivalent π model for long transmission can be represented by an equivalent Pi model, as shown in Fig. 4.

Length	Difference,%					
(mi)	$\Delta \mathbf{R}$	ΔX	$\Delta \mathbf{B}$			
10	0	0	0			
50	0.35	0.18	0			
100	1.43	0.71	0.35			
200	5.90	2.87	1.42			
300	14.09	6.62	3.20			
400	27.33	12.21	5.71			
500	48.34	20.03	8.98			

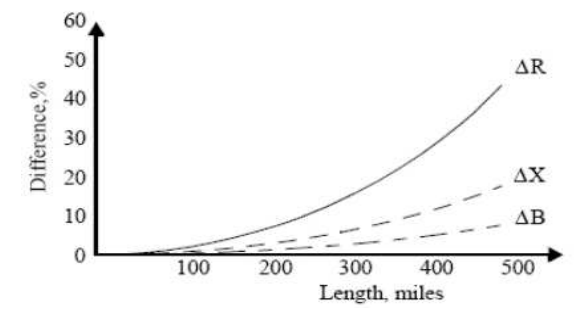


Fig. 3. Difference in line parameter with distributed and lumped modeling

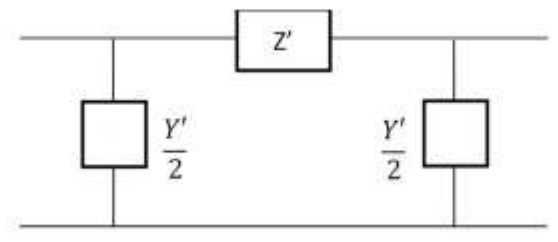


Fig. 4. Equivalent π model of long transmission lines.

The equivalent series impedance and shunt charging admittance for this modeling can be computed as:

$$Z' = zl \frac{\sinh(\gamma l)}{\gamma l} \tag{4}$$

$$Y' = yl \frac{\tanh(\gamma l/2)}{(\gamma l/2)}$$
 (5)

where γ represents the propagation constant defined as $\gamma = \sqrt{zy}$. The l denotes the length of the transmission line, while z and y are the series impedance and shunt admittance per unit length of the transmission line.

Thermal limit of a transmission line denoted as MVA_{max} can be determined through a calculation involving the line voltage, V_{line} , the maximum permissible current within the conductor, I_{max} , and the number of sub-conductors per phase, as depicted in Eq. (6).

$$MVA_{max} = \sqrt{3} \times V_{line} \times I_{max} \times b$$
 (6)

The line parameters and the maximum line loading limit, S_{in}^{max} , considered as 80% of the thermal limit, for the considered transmission line structure is given in Table III.

TABLE III. LINE PARAMETERS

kV	ACSR		MVA		
	Conductor	R (Ω/km)	L (mH/km)	C (nF/km)	limit
500	Macaw, 3 bundle	0.0228	0.878	12.975	2411

IV. POWER FLOW FORMULATION

Analyzing the power flow holds significant importance in the planning and designing of future power system expansions as well as optimizing the existing system's operation for optimal performance. It enables the identification of congestion areas, voltage violations, and line loading conditions, facilitates network reconfiguration, and ultimately contributes to the resilience and sustainability of power systems in the face of evolving energy demands, aiding new generations, and technological advancements.

The generalized equations for the load flow analysis are illustrated in Eq. (7) to Eq. (10).

$$I = Y_{hus}V \tag{7}$$

$$P_i + jQ_i = V_i I_i^* \tag{8}$$

$$P_{i} = |V_{i}| \sum_{n=1}^{N} |V_{n}| |Y_{in}| \cos(\theta_{in} - \delta_{i} + \delta_{n})$$
 (9)

$$Q_{i} = -|V_{i}| \sum_{n=1}^{n} |V_{n}| |Y_{in}| \sin(\theta_{in} - \delta_{i} + \delta_{n})$$
 (10)

where, $|Y_{in}|$ and θ_{in} are the magnitude and angle, respectively, of an element in the bus admittance matrix, |V| and δ denotes the magnitude and angle of the bus voltage, I represents the bus-injected current, and P and Q are the injected active and reactive power into the buses, respectively.

The power flow problem is subject to the following constraints.

Normal condition: $0.95 \le |V_i| \le 1.05 \ p.u.$ (11)

Contingency condition: $0.95 \le |V_i| \le 1.05 \ p. \ u.$ (12)

$$-0.3P_{gi} \le Q_{gi} \le 0.6P_{gi} \tag{13}$$

$$S_{in} \le S_{in}^{max} \tag{14}$$

Eqs. (11) and (12) are the constraints aimed at maintaining the voltage magnitude of all buses within acceptable limits during normal operating conditions and all single contingency scenarios, respectively. Eq. (13) ensures the reactive power generation by all generator units connected to the PV bus remains within the specified limit. The constraint outlined in Eq. (14) ensures that power flowing through the transmission line connecting two buses does not surpass their maximum capacity, determined by the thermal limit.

Contingency scenarios commonly occur in power systems, which makes it essential to ensure the system's operability under all single contingency conditions to maintain grid resilience, reliability, and robustness. The considered constraint in the TEP analysis typically includes the outage of transmission lines and transformers. However, this test system is created and made operable under all single contingencies considering the outage of the transmission line as a contingency component. For this analysis load flow Eqs. (7) - (10) and the constraints Eqs. (12) - (15) remains applicable.

V. POWER FLOW RESULT AND ANALYSIS

The power flow analysis was conducted using the Newton-Raphson method in the PSS/E 35.4 software. Generation and load data presented in Table II correspond to peak loading conditions. To analyze dominant and light loading conditions, all generation and load information from peak loading conditions were proportionately scaled and utilized. This approach ensures an accurate representation of system behavior across various operating conditions. Analysis was performed for normal and all single contingency conditions for three different loading conditions and the results are detailed in this section.

A. Peak Load: Normal Operating Conditions

The summarized power flow analysis results of the test system at peak load condition under normal operating conditions are presented in Table IV. The result shows that per unit voltage at all buses and reactive power generations at the generating unit connected to PV buses are within the defined ranges. Three maximum loaded lines are line 5-6, line 2-3, and line 6-9 with loading percentages of 32.52%, 32.50%, and 31.74%, all well below their maximum capacity.

B. Peak Load: Contingency Conditions

The operation of the test system at peak load under each contingency condition was tested by switching out individual transmission line and performing load flow analysis for each outage. The summarized load flow for each single contingency condition is summarized and presented in Table V. Each row of

the table corresponds to a different contingency condition, presenting the lowest voltage occurring bus and highest loading line along with their corresponding value. The result indicates a severe contingency occurs when one of the lines connecting bus 15 to bus 17 is out of operation. At this condition, the minimum voltage was observed at bus 17, with a magnitude of 0.907 p.u. The maximum loading of 53.40% was experienced in a line 6-9 when the other 6-9 line was not in service. It is noteworthy that the results for every single contingency met the voltage limit, line loading limit, and reactive power generation limits as stated in Eqs. (12) - (14). This signifies that the test system can effectively operate under all single contingency scenarios.

TABLE IV. SUMMARIZED LOAD FLOW ANALYSIS AT PEAK LOAD UNDER NORMAL OPERATING CONDITION

D "	Vol	tage	Gene	eration
Bus #	V p.u.	δ (deg.)	P _g (MW)	Qg (Mvar)
1	1.050	0.00	3321.2	-1382.6
2	1.045	-11.04	0.0	0.0
3	1.030	11.35	3600.0	177.8
4	1.050	-14.69	0.0	0.0
5	1.049	-18.32	0.0	0.0
6	1.030	3.52	3400.0	130.8
7	1.042	-18.29	0.0	0.0
8	1.040	-3.05	3600.0	-166.7
9	1.028	-13.62	0.0	0.0
10	1.030	-5.07	3600.0	-244.6
11	1.032	-16.97	0.0	0.0
12	1.050	-9.63	3600.0	-370.9
13	1.050	-4.08	3600.0	292.2
14	1.045	-1985	0.0	0.0
15	1.000	-6.06	3500.0	-436.8
16	1.046	-19.00	0.0	0.0
17	1.049	-21.71	0.0	0.0

TABLE V. SUMMARIZED RESULTS OF LOAD FLOW ANALYSIS AT PEAK LOAD FOR ALL SINGLE CONTINGENCIES

Line outage	Lowest	Lowest Voltage		st Line ng
	V p. u.	Bus#	% loading	Line
1–2 (1 line)	0.972	2	33.63%	1–7
1-4 (1 line)	0.932	4	36.33%	1-4
1–7 (1 line)	0.969	7	45.56%	1-7
2–3 (1 line)	0.949	2	49.76%	2-3
2–5	0.969	5	36.00%	1-7
3–6	1.000	15	38.59%	2-3
4–8 (1 line)	0.947	4	32.56%	6–9
5–6	0.935	5	39.85%	6–9
5–7	0.972	5	31.64%	6–9
5-10	0.938	5	39.05%	5–6
6–9 (1 line)	0.918	9	53.40%	6–9
7–11	0.984	11	32.50%	2-3
7–12	0.978	7	38.05%	11-13
8-11 (1 line)	0.956	11	39.50%	8-11
9-10	0.946	9	34.16%	6–9
9–15	0.978	9	34.04%	6–9
10-14 (1 line)	0.996	14	35.75%	10-14
11–13	0.953	11	37.62%	7 - 12
12-14 (1 line)	0.994	14	32.68%	6–9
12-16 (1 line)	0.954	16	32.67%	5–6
13–16 (1 line)	0.940	16	37.89%	11-13
14–15	1.000	15	34.27%	5–6
14–17	0.930	17	32.65%	2-3
15-17 (1 line)	0.907	17	36.54%	15-17

C. Dominant Load: Normal Operating Condition

The dominant loading was considered as the 60% loading of the peak loading condition. For the analysis of the test system at dominant loading conditions, the voltage of all generating units was set to 1.0 p.u. and a total of 2350 Mvar shunt reactor needed to be connected at different buses. The shunt reactor connected buses and their corresponding capacity is presented in Table VI.

TABLE VI. INFORMATION OF SHUNT REACTOR AT DOMINANT LOAD

Bus	2	4	5	7	8	10
Mvar	200	100	200	150	200	200
Bus	12	14	15	16	17	
Mvar	550	200	250	100	200	

The summarized load flow analysis of the test system under normal operating condition at the dominant load is shown in Table VII. The result shows that bus voltage, line loading, and reactive power generation by all generating units connected to PV buses are within their required thresholds, as outlined in Eqs. (11), (13) and (14).

TABLE VII. POWER FLOW ANALYSIS RESULT AT DOMINANT LOAD UNDER NORMAL OPERATING CONDITION

T "	Vol	tage	Generation		
Bus #	V p.u.	δ (deg.)	P _g (MW)	Q _g (Mvar)	
1	1.000	0.00	1945.3	-2030.25	
2	1.048	-6.85	0.0	0.0	
3	1.000	7.07	2160.0	-383.29	
4	1.044	-9.27	0.0	0.0	
5	1.050	-11.19	0.0	0.0	
6	1.000	1.95	2160.0	-520.87	
7	1.049	-11.32	0.0	0.0	
8	1.000	-1.75	2160.0	-594.42	
9	1.024	-8.29	0.0	0.0	
10	1.000	-2.87	2160.0	-641.17	
11	1.032	-10.45	0.0	0.0	
12	1.000	-5.55	2160.0	-642.18	
13	1.000	-2.13	2160.0	-410.40	
14	1.048	-12.06	0.0	0.0	
15	1.000	-3.71	2100.0	-587.97	
16	1.045	-11.63	0.0	0.0	
17	1.044	-13.12	0.0	0.0	

D. Dominant Load: Contingency Conditions

Similar to the contingency analysis conducted under peak load conditions, load flow analysis was also performed in the dominant load for each line outage, and specific outcomes of this analysis are summarized in Table VIII. It was found that the most critical contingency for the dominant loading condition occurred with the outage of line 5 – 6. Under this scenario, the minimum voltage was recorded as bus 5, with a magnitude of 0.938 p.u. Even in this most severe contingency, the voltage at all buses remained well above their lower limit. The other constraints such as reactive power generation limits and line loading under contingencies at dominant loading met specified thresholds.

E. Light Load: Normal and Contingency Conditions

The light loading condition was defined as 40% loading of the peak loading condition. All the generations and loads were scaled to 40% for the analysis of system operation at light loading conditions. To ensure operability under this light loading while meeting technical requirements such as bus voltage and reactive power generations, a total of 6800 Mvar shunt reactors needed to be connected to various buses. Details regarding the shunt reactors connected buses and their respective capacities are given in Table IX. All generating units were set to a voltage of 1.0 p.u. A load flow analysis was conducted under normal operating condition, and its results are presented in Table X. These results indicate that the per unit voltage of each bus and the limit for reactive generation are within their defined thresholds. Among all single contingency conditions, the minimum observed voltage remained comfortably above the threshold, at 0.963 p.u. when one 14-17 line was not in operation.

TABLE VIII. POWER FLOW ANALYSIS RESULT AT DOMINANT LOAD UNDER NORMAL OPERATING CONDITIONS

Line outage	Lowest	Voltage	The Highes Loadir	
	V p.u.	Bus#	% loading	Line
1–2 (1 line)	1.000	PV Bus	23.20%	1–7
1-4 (1 line)	0.989	4	22.72%	1-4
1-7 (1 line)	1.000	PV Bus	28.26%	1-7
2-3 (1 line)	0.949	PV Bus	31.42%	2-3
2–5	0.999	5	23.42%	5–6
3–6	1.000	PV Bus	26.20%	2-3
4–8 (1 line)	0.989	4	23.44%	1-7
5–6	0.935	5	25.66%	2-3
5–7	0.989	5	22.62%	2-3
5-10	0.938	PV Bus	25.33%	5–6
6–9 (1 line)	0.982	9	31.22%	6–9
7–11	0.986	11	23.30%	2-3
7–12	1.000	PV Bus	24.70%	11-13
8-11 (1 line)	0.998	11	25.22%	8-11
9–10	0.975	9	21.42%	6–9
9-15	0.981	9	23.06%	2-3
10-14 (1 line)	1.000	PV Bus	23.98%	10 - 14
11–13	1.000	PV Bus	25.13%	7 - 12
12-14 (1 line)	0.994	PV Bus	23.13%	2-3
12–16 (1 line)	0.999	16	23.53%	2-3
13-16 (1 line)	0.995	16	24.42%	11-13
14–15	1.000	PV Bus	24.08%	5–6
14–17	0.955	17	23.42%	2-3
15-17 (1 line)	0.969	17	22.86%	15-17

The comprehensive load flow analysis results for the proposed test system, conducted under normal operating conditions and in the presence of all single contingencies across three distinct loading scenarios, confirm compliance with the technical specifications stated in Eqs. (11) – (14). This ensures that the system is robust enough to withstand and operate effectively under a broad spectrum of load variations, ranging from light to peak loads, under normal and all different single contingencies.

TABLE IX. INFORMATION OF SHUNT REACTOR AT DOMINANT LOAD

Bus	2	3	4	5	6	7	8	9
Mvar	450	200	300	400	450	400	650	100
Bus	10	11	12	13	14	15	16	17

TABLE X. LOAD FLOW ANALYSIS RESULT AT LIGHT LOADING UNDER NORMAL OPERATING CONDITION

- "	Vol	tage	Gene	eration
Bus #	V p.u.	δ (deg.)	P _g (MW)	Qg (Mvar)
1	1.000	0.00	1287.3	-2117.8
2	1.050	-4.56	0.0	0.0
3	1.000	4.74	1440.0	-403.6
4	1.049	-6.20	0.0	0.0
5	1.050	-7.42	0.0	0.0
6	1.000	1.35	1440.0	-400.2
7	1.050	-7.52	0.0	0.0
8	1.000	-1.14	1440.0	-414.4
9	1.046	-5.43	0.0	0.0
10	1.000	-1.81	1440.0	-383.1
11	1.049	-6.94	0.0	0.0
12	1.000	-3.60	1440.0	-387.9
13	1.000	-1.35	1440.0	-417.1
14	1.050	-7.98	0.0	0.0
15	1.000	-2.34	1400.0	-372.8
16	1.047	-7.71	0.0	0.0
17	1.044	-8.66	0.0	0.0

An earlier version of this test system was presented in [8], however, the test system was for a single loading condition, peak load. We fixed this issue in the next papers [9, 10] where it works for other loading conditions as well. A second issue was that line parameters were obtained by multiplying their length by the per-length parameters and as highlighted in this paper, Fig. 3, it can lead to inaccuracies in calculating the line parameters. In this paper, we addressed this issue as well. These test systems were used to study a novel concept: using unconventional lines having high-power delivery [11] compared to conventional lines for transmission expansion planning (TEP) [12-15]. In addition to different transmission line design aspects that need to be studied for unconventional lines having high-power delivery like those done in [16-19], live line working may be challenging due to the interaction of maintenance personnel and those lines with unconventional bundle arrangements especially in freezing conditions [20-24].

VI. CONCLUSION

A high voltage, 500 kV, 17-bus test system has been introduced specifically for, but not limited to, transmission expansion planning (TEP), and all relevant information is presented in this paper. The system contains long transmission lines and is precisely modeled in a distributed manner to find accurate line parameters which makes the system more practical and reliable. The proposed test system can effectively operate under normal and all single contingency conditions at three different loading scenarios: peak load, dominant load, and light load, and meet all technical requirements. The operation of the test system for each condition has been validated by performing a comprehensive load flow analysis. For studies on transmission expansion planning, this system would be of great value.

REFERENCES

- [1] "International Energy Outlook U.S. Energy Information Administration (EIA)." [Online]. Available: https://www.eia.gov/outlooks/ieo/data.php
- [2] J. S. Heeter, B. K. Speer, and M. B. Glick, "International Best Practices for Implementing and Designing Renewable Portfolio Standard (RPS) Policies," NREL/TP--6A20-72798, 1507986, Apr. 2019.

- [3] E. Larson et al., "Net-Zero America: Potential Pathways, Infrastructure, and Impacts," interim Rep., Princeton University, Princeton, NJ, 2020.
- [4] "Power Systems Test Case Archive UWEE." [Online]. Available: https://labs.ece.uw.edu/pstca/
- [5] "Electric Grid Test Cases." [Online]. Available: https://electricgrids.engr.tamu.edu/electric-grid-test-cases/
- [6] "Power Cases Illinois Center for a Smarter Electric Grid (ICSEG)." [Online]. Available: https://icseg.iti.illinois.edu/power-cases/
- [7] H. Wei-Gang, "Study on conductor configuration of 500 kV Chang-Fang compact line," *IEEE Trans. Power Del.*, vol. 18, no. 3, pp. 1002–8, 2003.
- [8] B. Dhamala and M. Ghassemi, "A test system for transmission expansion planning studies meeting the operation requirements under normal condition as well as all single contingencies," *IEEE North American Power Symposium (NAPS)*, Asheville, NC, USA, 2023, pp. 1-5.
- [9] B. Dhamala and M. Ghassemi, "A test system for transmission expansion planning studies," *Electronics*, vol. 13, no. 3, p. 664, 2024.
- [10] B. Dhamala and M. Ghassemi, "A high voltage test system meeting requirements under normal and all single contingencies conditions of peak, dominant, and light loadings for transmission expansion planning studies," *IEEE Texas Power* and *Energy Conference (TPEC)*, College Station, TX, USA, February 12-13, 2024.
- [11] M. Ghassemi, "High surge impedance loading (HSIL) lines: A review identifying opportunities, challenges, and future research needs," *IEEE Trans. Power Delivery*, vol. 34, no. 5, pp. 1909-1924, Oct. 2019.
- [12] B. Dhamala and M. Ghassemi, "Comparative study of transmission expansion planning with conventional and unconventional high surge impedance loading (HSIL) lines," *IEEE Power & Energy Society General Meeting (PES GM)*, Seattle, WA, USA, 2024.
- [13] B. Dhamala and M. Ghassemi, "Unconventional high surge impedance loading (HSIL) lines and transmission expansion planning," *IEEE North American Power Symposium (NAPS)*, 2023, pp. 1-6.
- [14] B. Dhamala and M. Ghassemi, "Transmission expansion planning via unconventional high surge impedance loading (HSIL) lines," *IEEE North American Power Symposium (NAPS)*, 2023, pp. 1-6.
- [15] B. Porkar, M. Ghassemi, and M. A. Khan, "Transmission expansion planning (TEP)-based unconventional high surge impedance loading (HSIL) line design concept," *IEEE North American Power Symposium* (NAPS), Asheville, NC, USA, 2023, pp. 1-5.
- [16] M. A. Khan and M. Ghassemi, "Corona loss calculation for unconventional high surge impedance loading transmission lines," *IEEE North American Power Symposium (NAPS)*, 2023, pp. 1-6.
- [17] M. A. Khan and M. Ghassemi, "A new unusual bundle and phase arrangement for transmission line to achieve higher natural power," *IEEE North American Power Symposium (NAPS)*, 2023, pp. 1-5.
- [18] M. A. Khan and M. Ghassemi, "Calculation of audible noise and radio interference for unconventional high surge impedance loading (HSIL) transmission lines," *IEEE Conference Electrical Insulation Dielectric Phenomena (CEIDP)*, East Rutherford, NJ, USA, 2023, pp. 1-4.
- [19] M. A. Khan and M. Ghassemi, "A new method for calculating electric field intensity on subconductors in unconventional high voltage, high power density transmission lines," *IEEE Conf. Electrical Insulation Dielectric Phenomena (CEIDP)*, 2023, pp. 1-4.
- [20] M. Ghassemi, M. Farzaneh, and W. A. Chisholm, "Three-dimensional FEM electrical field calculation for FRP hot stick during EHV live-line work," *IEEE Trans. Dielectr. Electr. Insul.*, vol. 21, no. 6, pp. 2531– 2540, Dec. 2014.
- [21] M. Ghassemi, M. Farzaneh, and W. A. Chisholm, "A coupled computational fluid dynamics and heat transfer model for accurate estimation of temperature increase of an ice-covered FRP live-line tool," *IEEE Trans. Dielectr. Electr. Insul.*, vol. 21, no. 6, pp. 2628–2633, Dec. 2014.
- [22] M. Ghassemi and M. Farzaneh, "Coupled computational fluid dynamics and heat transfer modeling of the effects of wind speed and direction on temperature increase of an ice-covered FRP live-line tool," *IEEE Trans. Power Del.*, vol. 30, no. 5, pp. 2268–2275, Oct. 2015.
- [23] M. Ghassemi and M. Farzaneh, "Effects of tower, phase conductors and shield wires on electrical field around FRP hot stick during live-line work," *IEEE Trans. Dielectr. Electr. Insul.*, vol. 22, no. 6, pp. 3413– 3420, Dec. 2015.
- [24] M. Ghassemi and M. Farzaneh, "Calculation of minimum approach distances for tools for live working under freezing conditions," *IEEE Trans. Dielectr. Electr. Insul.*, vol. 23, no. 2, pp. 987–994, Apr. 2016.